Ecotoxicology and Environmental Safety 222 (2021) 112531

Contents lists available at ScienceDirect

Ecotoxicology and Environmental Safety

journal homepage: www.elsevier.com/locate/ecoenv

Arsenic trioxide induces expression of BCL-2 expression via NF-κB and p38 MAPK signaling pathways in BEAS-2B cells during apoptosis

Jing Tang [a,1], Chenjuan Yao [b,1], Yingqi Liu [a], Jiaming Yuan [a], Li Wu [a], Kazuo Hosoi [b,c,2], Shali Yu [a], Chunyan Huang [d], Haiyan Wei [a,*], Gang Chen [a,*]

[a] Department of Occupational Medicine and Environmental Toxicology, School of Public Health, Nantong University, Nantong 226019, Jiangsu, China
[b] Department of Molecular Oral Physiology, Institute of Health Biosciences, University of Tokushima Graduate School, Toku shima-Shi 770-8504, Tokushima, Japan
[c] Kosei Pharmaceutical Co. Ltd., Osaka-shi 540-0039, Osaka, Japan
[d] Department of Chronic Disease Prevention and Control, Suzhou Center for Disease Control and Prevention, Suzhou 215004, China

ARTICLE INFO

Edited by: Dr Yong Liang

Keywords:
Arsenic trioxide
BCL-2
Apoptosis
p38 MAPK
Phosphorylation
NF-κB

ABSTRACT

Inorganic arsenic compounds are environmental toxicants that are widely distributed in air, water, and food. B-cell lymphoma 2 (BCL-2) is an oncogene having anti-apoptotic function. In this study, we clarify that BCL-2, as a pro-apoptotic factor, participates in As_2O_3-induced apoptosis in BEAS-2B cells. Specifically, As_2O_3 stimulated the expression of BCL-2 mRNA and protein in a dose-dependent manner which was highly accumulated in the nucleus of BEAS-2B cell together with chromatin condensation and DNA fragmentation during apoptosis. Mechanistically, the process described above is mediated through the NF-κB and p38 MAPK signaling pathways, which can be abated by corresponding inhibitors, such as BAY11–7082 and SB203580, respectively. Additionally, BAY11–7082, actinomycin D, and cycloheximide have inhibitory effects on As_2O_3-induced expression of BCL-2 mRNA and protein, and restore the cell viability of BEAS-2B cells. Suppression of BCL-2 protein activation by ABT-199 also restored viability of BEAS-2B cell in As_2O_3-induced apoptosis. Furthermore, As_2O_3 increased the level of BCL-2 phosphorylation. These results suggest that in BEAS-2B cells, As_2O_3-induced apoptosis is mainly dominated by BCL-2 upregulation, nuclear localization and phosphorylation. The study presented here provides a novel insight into the molecular mechanism of BCL-2-induced apoptosis.

1. Introduction

Inorganic arsenic is found widely in nature in the form of oxides and sulfides. The two main oxidative states of arsenic are pentavalent arsenate (AsV) and trivalent arsenite (AsIII). AsIII is much more toxic than AsV (Hughes et al., 2011). Inorganic arsenic compounds are environmental toxicants that are widely distributed in air, water, and food (Hughes et al., 2011). Epidemiological studies have suggested that exposure to low or moderate levels (10–300 μg/L) of arsenic via drinking water may lead to adverse human health effects and chronic diseases, including dermal diseases, cardiovascular disorders, neurological disorders, diabetes, respiratory complications, liver and kidney diseases (Abdul et al., 2015). Inorganic arsenic in the air can be absorbed by the respiratory system and cause lung dysfunction, skin lesions, neuropathy, nephrotoxicity, and hepatic dysfunction (Liu et al., 2002). In some areas, the coals contain high concentrations of arsenic. These coals are burned inside the home as a source of energy, and the concentrations of arsenic are measured 20–400 μg/m^3 in the indoor air (Liu et al., 2002). The concentration of arsenic in the air of the workshop can be as high as several milligrams per cubic meter (WHO, 2001). Therefore, exposure to high concentrations of arsenic in the air may induce damage to the lung epithelial cells.

Apoptosis, a type of programmed cell death, will cause the morphological changes of cells, such as cell shrinkage, nuclear fragmentation, DNA fragmentation, and chromatin condensation (Taylor et al., 2008). The two well-known activation mechanisms of apoptosis are the intrinsic and the extrinsic pathways (Carneiro and El-Deiry, 2020). The intrinsic pathway of apoptosis is activated by intracellular signals released from the intermembrane space of mitochondria when cells are exposed to stress. The extrinsic pathway of apoptosis is

* Corresponding authors.
E-mail addresses: why1987@ntu.edu.cn (H. Wei), chengang@ntu.edu.cn (G. Chen).
[1] These authors contributed equally to this work.
[2] Professor emeritus, Tokushima University.

https://doi.org/10.1016/j.ecoenv.2021.112531
Received 6 May 2021; Received in revised form 4 July 2021; Accepted 15 July 2021
Available online 21 July 2021

activated by the binding of extracellular ligands to the cell-surface death receptor, leading to the formation of the death-inducing signaling complex (Taylor et al., 2008; Carneiro and El-Deiry, 2020).

The intrinsic pathway is reported to be controlled by members of the BCL-2 protein family (Czabotar et al., 2014). Based on functional studies, the BCL-2 family members containing one or more BCL-2 homology (BH) domains are grouped into 3 classes: proteins with similar globular structure with 4 BH regions (BH1, BH2, BH3, and BH4), proteins with BH3 domain only, and effector proteins, which contain one or more BH regions. Proteins with BH3 domain only (e.g. BID, BIM, PUMA, BAD, and NOXA) are pro-apoptotic, whereas the BCL-2 proteins with multi-BH domains can be either anti-apoptotic (e.g. BCL-2, BCL-w, BCL-xL, MCL-1, and BFL1/A1) or pro-apoptotic (e.g. BAX and BAK). The role of BCL-2 protein in anti-apoptosis is important as it binds to BAX and other pro-apoptotic proteins, thereby inhibits apoptosis (Singh et al., 2019). Once the binding between BCL-2 and the pro-apoptotic protein is dissociated, BCL-2 can be degraded by diverse stimuli, significantly reducing the expression level of BCL-2 protein in apoptosis (Siddiqui et al., 2015; Edison et al., 2017). Nevertheless, some researchers have reported that BCL-2 has both anti-apoptotic and pro-apoptotic functions, depending on the expression level and distribution of BCL-2 (Shinoura et al., 1999; Massaad et al., 2004; Portier and Taglialatela, 2006; Hanson et al., 2008). The anti-apoptotic function of BCL-2 has been investigated mainly in mitochondria, where chaperone FKBP38 interacts with shuttles BCL-2 and locates in the outer mitochondrial membrane (Shirane and Nakayama, 2003; Wang et al., 2005). Perturbation of the above complex formation by FKBP38 siRNA alters the intracellular localization of BCL-2 and interferes with its anti-apoptotic function (Shirane and Nakayama, 2003; Portier and Taglialatela, 2006; Choi et al., 2013). In addition, phosphorylation of BCL-2 is significantly increased in drug-mediated apoptosis, including that under the action of paclitaxel, vincristine, and vinblastine (Haldar et al., 1996; Srivastava et al., 1998, 1999). Phosphorylated BCL-2 was found to be translocated into the nucleus in aspirin-mediated apoptosis (Choi et al., 2013).

Inorganic arsenic has been found to induce apoptosis via activation of the intrinsic and/or extrinsic pathways in several cellular systems (Kumar et al., 2014; Dua et al., 2016; Rahman et al., 2018). It has been previously demonstrated that As_2O_3 upregulates the expression level of proteins in the pro-apoptotic BCL-2 family, while downregulates the expression level of proteins in the anti-apoptotic BCL-2 family, triggering the intrinsic apoptosis (Banerjee et al., 2008; King et al., 2016). Surprisingly, we found that As_2O_3 increased BCL-2 expression in a dose-dependent manner which was in contradiction with these published literature. Thus, the aim of this study was to investigate the mechanisms of increased BCL-2 expression in As_2O_3 induced-apoptosis in human bronchial epithelial cells (BEAS-2B).

2. Materials and methods

2.1. Reagents and antibodies

N-acetyl-L-cysteine (NAC), actinomycin D (Act D), BAY11–7082, and cycloheximide (CHX) were procured from Sigma-Aldrich (St. Louis, MO, USA). PD98059 and SP600125 were ordered from Cell Signaling Technology Comp. (Cell Signaling Technology, Danvers, MA, USA). SB203580 and ABT-199 were purchased from Target Molecule Corp. (TargetMol, Boston, MA, USA). As_2O_3 was obtained from Merck and Co., Inc., (Kenilworth, New Jersey, USA) with a purity of more than 99.95%. As_2O_3 was dissolved in 1 N NaOH at 100 mM and further diluted to 5 mM in PBS as a stock solution. Phos-tag™ Acrylamide was received from Wako Pure Chemical Industries (Osaka, Japan). RNAiso Plus reagent, the PrimeScript II RT enzyme kits, and PCR amplification kits were bought from Takara Biotechnology Dalian Co. Ltd. (Takara, Dalian, China). A lactate dehydrogenase (LDH) analysis kit was procured from Nanjing Jiancheng Bioengineering Institute (Nanjing, China). The Cell Counting Kit-8 (CCK-8) was ordered from Dojindo Laboratories (Kumamoto, Japan). The enhanced chemiluminescence (ECL) detection kits were offered by Millipore (Bedford, MA, USA). Protease inhibitor cocktail tablets were purchased from Roche Applied Science (Indianapolis, IN, USA). Phosphatase inhibitor cocktail A was purchased from Beyotime Biotechnology (Shanghai, China). Anti-cleaved caspase-3 (ab2302) was purchased from Abcam Comp. (Abcam, Cambridge, UK). Anti-BCL-2 (12789–1-AP), anti-BAX (50599–2-lg), anti-Lamin A/C (10298–1-AP), and anti-β-tubulin (10094–1-AP) were procured from Proteintech Comp (Proteintech, Chicago, USA). Anti-poly (ADP-ribose) polymerase (PARP; 9542), anti-ERK1/2 (4695), anti-p-ERK1/2 (phosphorylated at Thr202/Tyr204, 4370), anti-JNK (9358), anti-p-JNK (phosphorylated at Thr183/Tyr185, 9255), anti-p38 MAPK (8690), and anti-p-p38 MAPK (phosphorylated at Thr180/Tyr182, 4511) were ordered from Cell Signaling Technology Comp. Anti-NF-κB p65 antibody (YM3111) was purchased from Immunoway Comp (Immunoway, Newark, DE, USA). Anti-β-actin (A3854) was purchased from Sigma-Aldrich Comp.

2.2. Cell culture and treatments

BEAS-2B cells were offered by the Cell Bank of the Chinese Academy of Sciences (Shanghai, China). The BEAS-2B cell line is derived from a human bronchial epithelium and has been extensively used as an in vitro human non-tumorigenic lung epithelial cell model in a large variety of studies. Therefore, BEAS-2B cells were used to study the molecular mechanism of arsenic-induced damage and apoptosis to the respiratory epithelial cells in this study. BEAS-2B cells were cultured in DMEM/F-12 medium (Corning, Manassas, VA, USA) supplemented with 10% fetal calf serum (Gibco, New York, USA) and penicillin-streptomycin (100 units/mL, Beyotime, Shanghai, China). Cells were maintained in a 37 °C incubator under a humidified atmosphere of 95% air and 5% CO_2. To explore the mechanism underlying the toxicity induced by As_2O_3, BEAS-2B cells were first cultured in the presence of various inhibitors for 30 min, followed by treatment with 2.0 μM As_2O_3 for 24 h; the inhibitor employed for each test was either 5.0 mM NAC, 10 μM CHX, 10 μM BAY 11–7082, 2 μg/mL Act D, 20 μM PD98059, 25 μM SP600125, 10 μM SB203580 or ABT-199.

2.3. Cell viability assay

The cytotoxicity of As_2O_3 to BEAS-2B cells was measured using a CCK-8 assay. Cells were spread in a 96-well plate at a density of 1×10^4 cells/well overnight. Subsequently, cells were incubated with different doses of As_2O_3 for 24 h or with 2.0 μM As_2O_3 for various lengths of time (0–72 h). After As_2O_3 treatment, each well was incubated with a 10.0 μL of CCK-8 solution for another 2 h in the dark followed by recording of the absorbance at 450 nm by use of BioTek ELX800, a microplate reader (BioTek Instruments, Winooski, VT, USA). The results are expressed as percentages relative to the value of untreated cells, which were regarded as having 100% viability.

2.4. LDH leakage assay

BEAS-2B cells were incubated with or without 2.0 μM As_2O_3 for 24 h. The culture medium was collected, and centrifuged at 100 g and 4 °C for 5 min to remove dead cells and/or cell debris. The LDH content in the culture supernatant was measured with a microplate reader using a LDH analysis kit following the manufacturer's instructions. Results are expressed as percentages relative to the value of untreated cells, which were regarded as having 100% viability.

2.5. Total RNA extraction, semi-quantitative reverse transcription and polymerase chain reaction (RT-PCR) analysis

Total RNA (2.5 μg aliquot) extracted from BEAS-2B cells by RNAiso

Plus reagent was reverse-transcribed into cDNA using a PrimeScript II RT Enzyme kit. BCL-2 mRNA was amplified using 5′-GACTTCGCCGAGATGTCCAG-3′ as the forward primer and 5′-TCACTTGTGGCCCAGATAGG-3′ as the reverse primer; BAX mRNA was amplified using 5′-CGTCCACCAAGAAGCTGAGCG-3′ as the forward primer and 5′-AGCACTCCCGCCACAAAGATG-3′ as the reverse primer; FKBP38 mRNA was amplified using 5′-GCTGACTCCAAGTACTGCTA-3′ as the forward primer and 5′-CAGACAATTCACCTTCAACT-3′ as the reverse primer. Additionally, β-actin mRNA used as an internal standard was amplified as reported (Liu et al., 2020.) using the same set of forward and reverse primers. PCR was conducted in a thermal cycler for 31 cycles (BCL-2), 28 cycles (BAX), 25 cycles (FKBP38), 21 cycles (β-actin). Each cycle consisted of denaturation at 94 °C for 30 s, annealing at 59 °C (BCL-2), or 61 °C (BAX), or 56 °C (FKBP38, β-actin) for 30 s, and extension at 72 °C for 60 s. The final extension time at 72 °C was 10 min. The reaction products were electrophoresed in ethidium bromide (0.5 μg/mL)-containing 2% agarose gels. The gels were visualized using a Bio-Rad Gel Doc™ EZ imager with a Bio-Rad Power Pac HC power supply (Hercules, CA, USA), and the band intensity was quantified by Image J software.

2.6. Western blotting

For total protein extracts, BEAS-2B cells were lysed in RIPA lysis buffer. Lysate was centrifuged to obtain the supernatant, while the nuclear and cytoplasmic fractions were separated by using a nuclear and cytoplasmic extraction kit (ComWin Biotech, Jiangsu, China) following the manufacturer's instructions. The protein concentration in each sample was quantified using the standard bicinchoninic acid protein assay.

Western blotting was performed following the standard procedure as described previously (Liu et al., 2020). Briefly, the protein in samples was denatured with SDS at 95 °C, separated via SDS-polyacrylamide gel electrophoresis (SDS-PAGE), and transferred to a polyvinylidene difluoride membrane (Immobilon-P, Merck KGaA, Darmstadt, Germany). Membranes were blocked with skimmed milk or bovine serum albumin for 2 h at room temperature and incubated at 4 °C overnight with specific primary antibodies against cleaved caspase-3 (1:500), PARP (1:1000), BCL-2 (1:1000), BAX (1:4000), Lamin A/C (1:1000), β-tubulin (1:1000), ERK1/2 (1:1000), p-ERK1/2 (1:1000), JNK (1:1000), p-JNK (1:1000), p38 MAPK (1:1000), p-p38 MAPK (1:1000), and β-actin (1:40,000). Finally, the membranes were incubated with goat anti-rabbit or mouse IgG secondary antibody coupled with horseradish peroxidase. The reactions were detected using an ECL assay, and visualized using a Tanon 5500 imaging system (Tannon, Shanghai, China). The band intensity was quantitatified by Image J software.

2.7. Phos-tag gel assay

BEAS-2B cells were treated with or without As_2O_3 for 24 h. Protein samples from these cells were prepared as described by Liu (Liu et al., 2020). Phos-tag gel assay was described previously (Kinoshita et al., 2009). Briefly, 20 μg of protein was loaded on 20 μM Phos-tag™ Acrylamide gel. After electrophoresis, Phos-tag Acrylamide gels were soaked in a transfer buffer containing 5 mM EDTA for 20 min. This step was repeated 3 times with gentle agitation to eliminate the manganese ions from the gel. Next, the gel was soaked in a transfer buffer without EDTA for 10 min with gentle agitation. The proteins were electrophoretically transferred to PVDF membranes in the transfer buffer without SDS/EDTA. The other steps were the same as regular Western Blotting experiments.

2.8. Immunofluorescence staining

For immunofluorescence staining, cells were grown on coverslips and fixed with 4% paraformaldehyde in phosphate-buffered saline (PBS) at 4 °C for 20 min, then the cells were treated with NH_4Cl (quenching of aldehyde group), permeabilized by Triton X-100, and blocked with bovine serum albumin. They were next incubated with rabbit polyclonal anti-BCL-2 antibody (1:100) or mouse monoclonal anti-NF-κB p65 antibody (1:100) at room temperature for 2 h. The cells were washed with PBS and reacted at 37 °C for 1 h with anti-rabbit IgG or anti-mouse IgG, both conjugated with Alexa Fluor 488. Nuclei were stained with 5 μg/mL Hoechst 33342 (Sangon Biotech., Shanghai, China) or 0.5 μg/mL DAPI (Beyotime, Shanghai, China) for 30 min. Images were collected using a Leica fluorescence microscope.

2.9. Statistical analyses

Data obtained from at least 3 independent experiments, each performed with at least 3 biological replicates. The results were expressed as the mean ± standard deviation of the mean (SEM) of 3 independent experiments. Two groups were compared using Student's two-tailed *t*-test. When more than one group was compared with one control, statistical significance was assessed using one-way ANOVA with a Dunnett's post-hoc test. The p value less than 0.05 was considered to be statistically significant.

3. Results

3.1. As_2O_3 induces apoptosis in BEAS-2B cells

The BEAS-2B cell line was originally established as an immortalized but non-tumorigenic epithelial cell line from the human bronchial epithelium. Therefore, it has been used in a large variety of studies as an in vitro cell model of lung injury. To determine whether BEAS-2B cells undergo apoptosis following the treatment with As_2O_3, the CCK-8 assay was applied first to evaluate the cytotoxicity of As_2O_3. When BEAS-2B cells were cultured in the presence of As_2O_3 at the concentration range of 0.5–4.0 μM for 24 h, an obvious reduction in cell viability was observed at concentrations of 1.0, 1.5, 2.0, and 4.0 μM (Fig. 1a). In addition, when BEAS-2B cells were treated with 2.0 μM of As_2O_3 for 12, 24, 48, 60 and 72 h, cell viability decreased in correlation with the incubation time (Fig. 1b). The results of the CCK-8 assay demonstrated that As_2O_3 significantly decreased the viability of BEAS-2B cells in a dose- and time-dependent manner (Fig. 1a and b). When the structure of plasma membrane is destroyed upon necrosis or apoptosis, LDH is released into the culture medium. Consequently, an increased level of LDH activity was measured in the culture medium after BEAS-2B cells were exposed to 2.0 μM As_2O_3 for 24 h (Fig. 1c).

Apoptosis is generally characterized by a series of morphological events such as shrinkage in the sizes of cells and nuclei, chromatin condensation, and DNA fragmentation. Therefore, we further examined the morphology of the nucleus in control and As_2O_3-treated cells using Hoechst 33342 staining. Compared to normal cells, nucleus shrinkage, chromatin condensation, and brighter fragments were observed in apoptotic cells. Specifically, in the control group and cells treated with 0.5 μM As_2O_3, the nuclei were stained weakly with a homogeneous blue color. However, in cells treated with 2.0 μM As_2O_3, the nuclei were well-stained and illustrated a strong blue color with shrunken morphology, suggesting chromatin condensation and nuclear fragmentation (Fig. 1d). Since caspase-3 is an essential regulator in the signal transduction pathway of apoptosis and the activation of caspase-3 triggers the PARP cleavage, caspase-3 is served as one of the common markers for apoptosis analysis. To further confirm whether As_2O_3 could induce apoptosis in BEAS-2B cells, the levels of cleaved caspase-3 and cleaved PARP proteins were assessed using Western blotting. As shown in Fig. 1E, the levels of cleaved caspase-3 and PARP protein were significantly upregulated in cells incubated with 2.0 μM and 4.0 μM As_2O_3 for 24 h. In contrast, the expression levels of either cleaved caspase-3 or PARP protein were not changed in the group of cells treated with 0.5 μM As_2O_3 (Fig. 1e). Altogether, the above results approved that As_2O_3

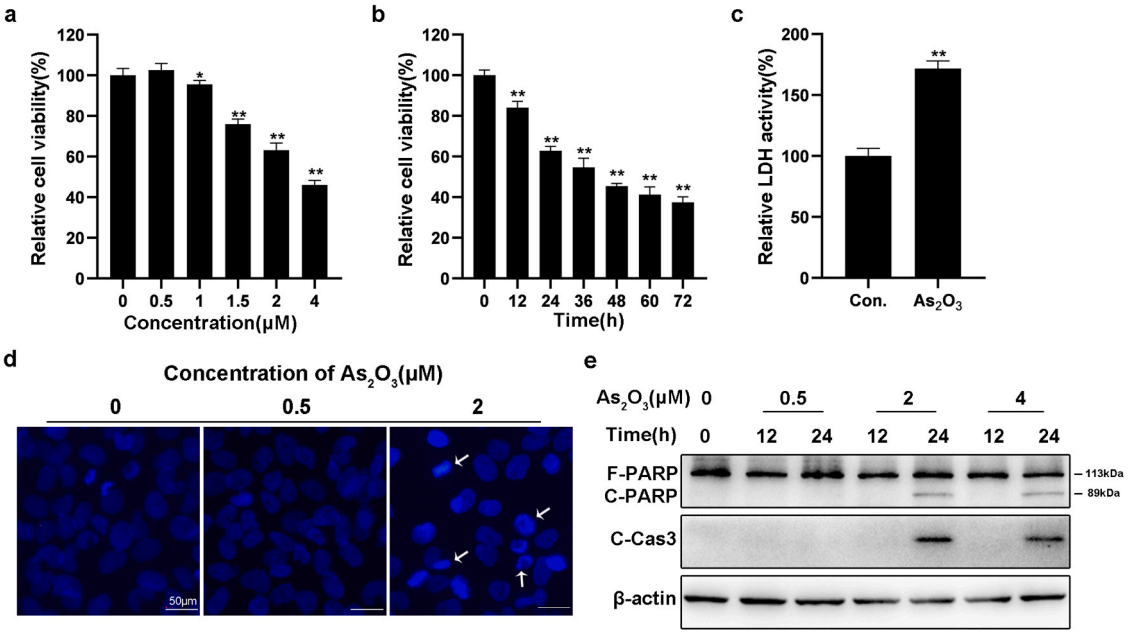

Fig. 1. Effects of As_2O_3 on the viability, nuclear morphology, and levels of apoptosis-related proteins in BEAS-2B cells. a. BEAS-2B cells were incubated with various concentrations of As_2O_3 for 24 h. b. BEAS-2B cells were incubated with 2.0 μM As_2O_3 for the indicated times. The cell viability was measured in a CCK-8 assay. c. BEAS-2B cells were incubated with or without 2.0 μM As_2O_3 for 24 h, and LDH activity in the culture supernatant was detected. In Fig. 1a, b, c, data were shown as the mean ± SEM of 3 independent experiments. * $p < 0.05$ and * * $p < 0.01$ compared to the control (without As_2O_3). d. BEAS-2B cells incubated with the indicated concentrations of As_2O_3 for 24 h were stained with Hoechst 33342. Specimens were observed under a fluorescence microscope. Arrows indicate shrunken, condensed, and/or fragmented nuclei as markers of apoptosis. The bar represents 50 μm. e. BEAS-2B cells were incubated with various concentrations of As_2O_3 for 12 or 24 h. Cell lysates were subjected to SDS-PAGE/immunoblotting using an anti-cleaved caspase-3 antibody, anti-PARP antibody, and anti-β-actin antibody. The blots represent one of 3 independent experiments. F-PARP, full length-poly (ADP-ribose) polymerase; C-PARP, cleaved-poly (ADP-ribose) polymerase; C-Cas3, cleaved caspase-3.

indeed induced cytotoxicity and apoptosis in BEAS-2B cells.

3.2. As_2O_3 stimulates expression of the BCL-2 mRNA and protein in BEAS-2B cells

In general, the BCL-2 protein is downregulated by the ubiquitin proteasome system during apoptosis (Edison et al., 2017). To verify whether As_2O_3 affects the BCL-2 mRNA and protein expression, BEAS-2B cells were incubated with different concentrations of As_2O_3 ranged from 0.25 to 2.0 μM for different periods. Intriguingly, both mRNA and protein levels of BCL-2 raised after treatment with As_2O_3 in a dose-dependent way (Fig. 2a and b). Meanwhile, as demonstrated in Fig. 2c and d, the expression levels of BCL-2 mRNA and protein increased in a time-dependent manner in BEAS-2B cells treated with 2.0 μM As_2O_3, respectively. As gene expression is regulated at the transcriptional and post-transcriptional levels, here Act D, a transcription inhibitor that is widely used in mRNA stability assays, was used to investigate its effect on the synthesis of BCL-2 mRNA. As illustrated in Fig. 2e, the treatment of cells with 2 μg/mL Act D for 3, 6, 12, and 24 h reduced the BCL-2 mRNA level by 10%, 31%, 46%, and 54%, respectively. Furthermore, the upregulation of the BCL-2 mRNA level by 2.0 μM As_2O_3 was completely blocked in the presence of Act D (Fig. 2e). The elevation of the BCL-2 protein level was also inhibited by Act D (Fig. 2f). Comparing the effect of Act D on mRNA levels between the control and As_2O_3-treated groups, it is suggested that As_2O_3-participated BCL-2 upregulation through transcriptional regulation. In addition, CHX, a protein synthesis inhibitor, significantly inhibited the As_2O_3-stimulated BCL-2 protein expression (Fig. 2g).

3.3. As_2O_3 increases BCL-2 expression through NF-κB activation and the p38 MAPK pathway in BEAS-2B cells

To determine whether As_2O_3 increases BCL-2 expression through NF-κB activation in BEAS-2B cells, cell immunostaining strategy was applied using anti-NF-κB p65 antibody. The results indicated that NF-κB was translocated from the cytoplasm into the nucleus upon 2.0 μM As_2O_3 treatment (Fig. 3a). Incubation with BAY11–7082 (10 μM), an NF-κB inhibitor, partially inhibited the As_2O_3-stimulated upregulation of BCL-2 mRNA and protein in BEAS-2B cells, respectively (Fig. 3b and c).

We have previously shown that As_2O_3 activates the MAPK pathway in a process mediated by reactive oxygen species in BEAS-2B cells (Liu et al., 2020). In this study, we found that 2.0 μM As_2O_3 significantly enhanced the phosphorylation levels of ERK1/2, JNK, and p38 MAPK in BEAS-2B cells (Fig. 3d). However, only SB203580, a p38 MAPK inhibitor, partially inhibited As_2O_3-induced BCL-2 mRNA and protein expression. PD98059, an ERK1/2 inhibitor and SP600125, a JNK inhibitor, showed no effect on the expression levels of BCL-2 mRNA and protein stimulated by As_2O_3 (Fig. 3e and f). These results suggested that As_2O_3 increased the expression levels of BCL-2 mRNA and protein through the NF-κB and p38 MAPK pathways.

3.4. The newly synthesized BCL-2 protein and its phosphorylation induced by As_2O_3 is located at the nucleus and associated with apoptotic chromatin condensation

Previous studies have shown that nuclear localization of BCL-2 is associated with apoptosis (Portier and Taglialatela, 2006; Choi et al., 2013). We therefore tested the effect of As_2O_3 on localization of BCL-2 in BEAS-2B cells. BCL-2 was located at the cytoplasm and nucleus in BEAS-2B cells before As_2O_3 treatment. Moreover, the BCL-2 protein level in the nucleus was much higher than that in the cytoplasm (Fig. 4a). After incubation with 2.0 μM As_2O_3 overnight, the fluorescence signal that was correlated with the amount of BCL-2 protein, significantly increased in the cytoplasm and nucleus. Furthermore, NAC, an antidote to As_2O_3 and a reactive oxygen species scavenger,

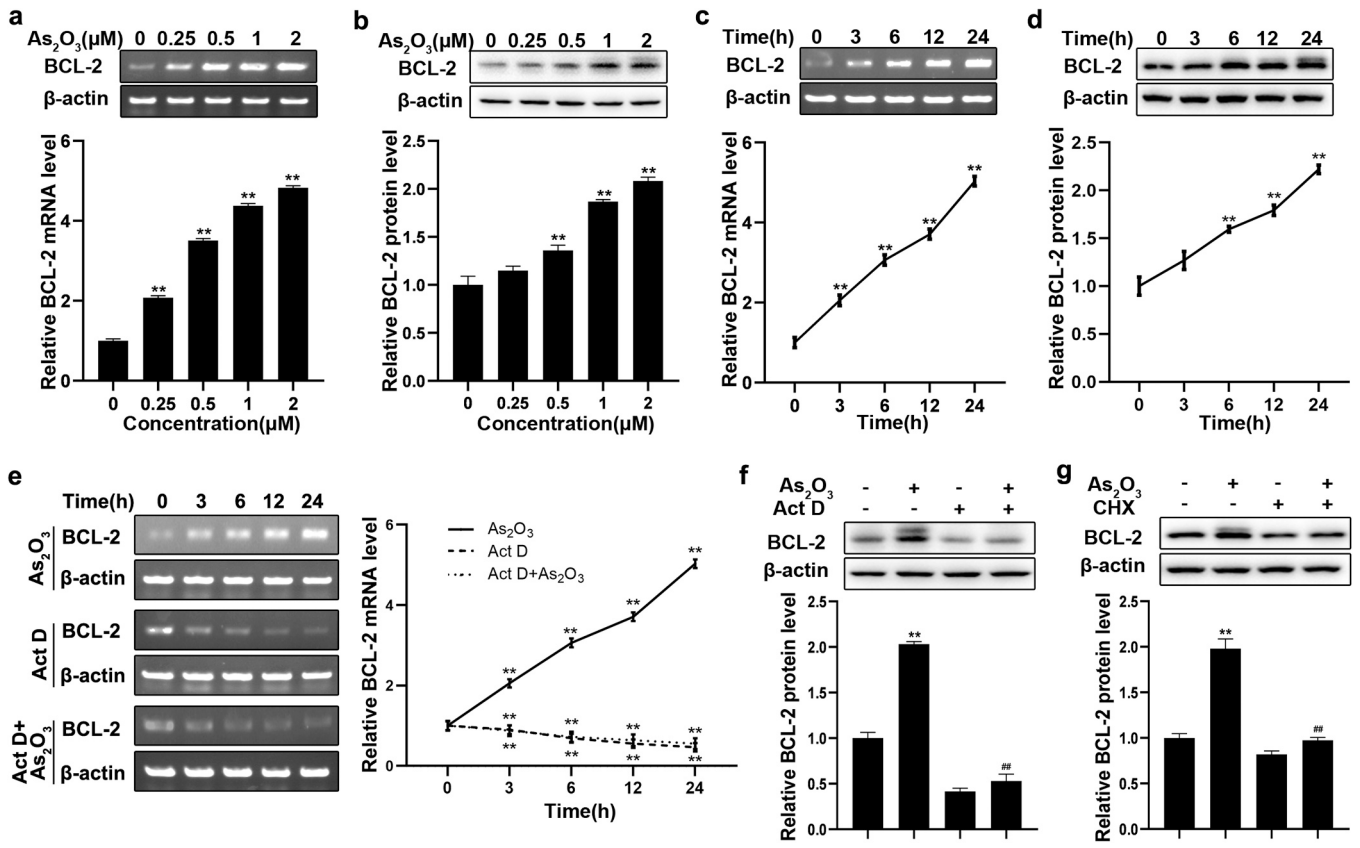

Fig. 2. Induction of expression of BCL-2 mRNA and protein by As_2O_3. BEAS-2B cells were incubated with various concentrations of As_2O_3 for 24 h. a. The expression of BCL-2 mRNA was measured using semi-quantitative RT-PCR analysis. b. The expression of BCL-2 protein was detected by Western blotting analysis. BEAS-2B cells were incubated with 2.0 μM As_2O_3 for the indicated time points. c. The expression of BCL-2 mRNA was measured by semi-quantitative RT-PCR analysis. d. The expression of BCL-2 protein was detected by Western blotting analysis. e. BEAS-2B cells were incubated with or without 2 μg/mL Act D for 30 min; 2.0 μM As_2O_3 was then added for the times indicated prior to RNA extraction. BCL-2 mRNA was measured using semi-quantitative RT-PCR analysis. BEAS-2B cells pretreated with 2 μg/mL Act D (f) or 10.0 μM CHX (g) for 30 min incubated with or without 2.0 μM As_2O_3 for 24 h; the level of BCL-2 protein in cell lysates was detected using Western blotting analysis. The band intensities representing BCL-2 protein expression levels were quantitated using the Image J Gel Analysis program and normalized by the intensity of the β-actin internal control. $^{**}p < 0.01$, significantly different from the control group; $^{\#\#}p < 0.01$, significantly different from the As_2O_3-treatment group.

completely inhibited As_2O_3-induced BCL-2 accumulation in the nucleus, whereas BAY11–7082 and SB203580 only partially inhibited the nuclear accumulation of As_2O_3-induced BCL-2 protein (Fig. 4a). BCL-2 protein increased in the cytoplasm and nucleus by As_2O_3 was also detected via subcellular fractionation analyses (Fig. 4b).

To further explore the relationship between BCL-2 elevation and nuclear morphology, BCL-2 nuclear accumulation, chromatin condensation, and DNA fragmentation were studied. Together with enhanced accumulation of BCL-2 protein in the nucleus upon As_2O_3 exposure, chromatin was condensed and nucleus was fragmented (Fig. 4a). NAC also decreased the level of BCL-2 protein in the cytoplasm and nucleus in BEAS-2B cells (Fig. 4b). BCL-2 is phosphorylated at plural serine/threonine sites (S70, T56, T69, T74, S87) within a nonstructural loop that links the BH3 and BH4 domains in response to multiple treatments. Microtubule injuries also induce mobility shifts in BCL-2 by phosphorylation of serine and threonine residues (Blagosklonny, 2001). Therefore, we subsequently analyzed the phosphorylation of BCL-2 protein induced by As_2O_3 in BEAS-2B cells. Phos-tag SDS-PAGE displayed 3 bands in proteins of BCL-2 (Fig. 4c), in which the upper and middle bands belonged to phosphorylated (P) species, while the lower band belonged to a non-phosphorylated (non-P) species. Beyond that, levels of phosphorylated BCL-2 protein increased dose-dependently after As_2O_3 treatment (Fig. 4c). In healthy cells, BCL-2 interacts with pro-apoptotic protein BAX on the surface of the mitochondrial outer membrane. During apoptosis, the levels of BAX mRNA and protein increased. We checked the expression of BAX in BEAS-2B cells treated with As_2O_3. No obvious variation was observed in the expression level of BAX mRNA and protein (Fig. 4d). FKBP38 binds BCL-2 and anchored it to the mitochondrial membrane to perform the anti-apoptotic effect. When the balance between FKBP38 and BCL-2 in the cell is disturbed, BCL-2 is translocated into the nucleus and induces apoptosis (Portier and Taglialatela, 2006). Accordingly, we aimed to determine whether As_2O_3 regulates FKBP38 expression. The result showed that the level of FKBP38 mRNA expression was not affected by As_2O_3 in the dose range of 0.25–2 μM (Fig. 4e).

In summary, the above results suggest that As_2O_3-induced accumulation and phosphorylation of BCL-2 in the nucleus may cause nuclear envelope destruction and chromatin condensation in BEAS-2B cells.

3.5. *Inhibition of As_2O_3-induced BCL-2 expression improves the viability of BEAS-2B cells*

The above findings demonstrate that As_2O_3-induced apoptosis is related to the upregulation and nuclear localization of BCL-2 protein. Therefore, we next evaluated the viability of BEAS-2B cells when BCL-2 expression was inhibited. BEAS-2B cells were pretreated with NAC, BAY11–7082, SB25038, Act D, or CHX for 30 min. The cells were then treated with 2.0 μM As_2O_3 for another 24 h and followed by a cell viability measurement using CCK-8 assay. As shown in Fig. 5a, cell viability was completely restored with NAC, and partially restored with BAY11–7082, SB25038, Act D, or CHX. To further examine the effects of these drugs, the protein levels of cleaved caspase-3 were assessed using

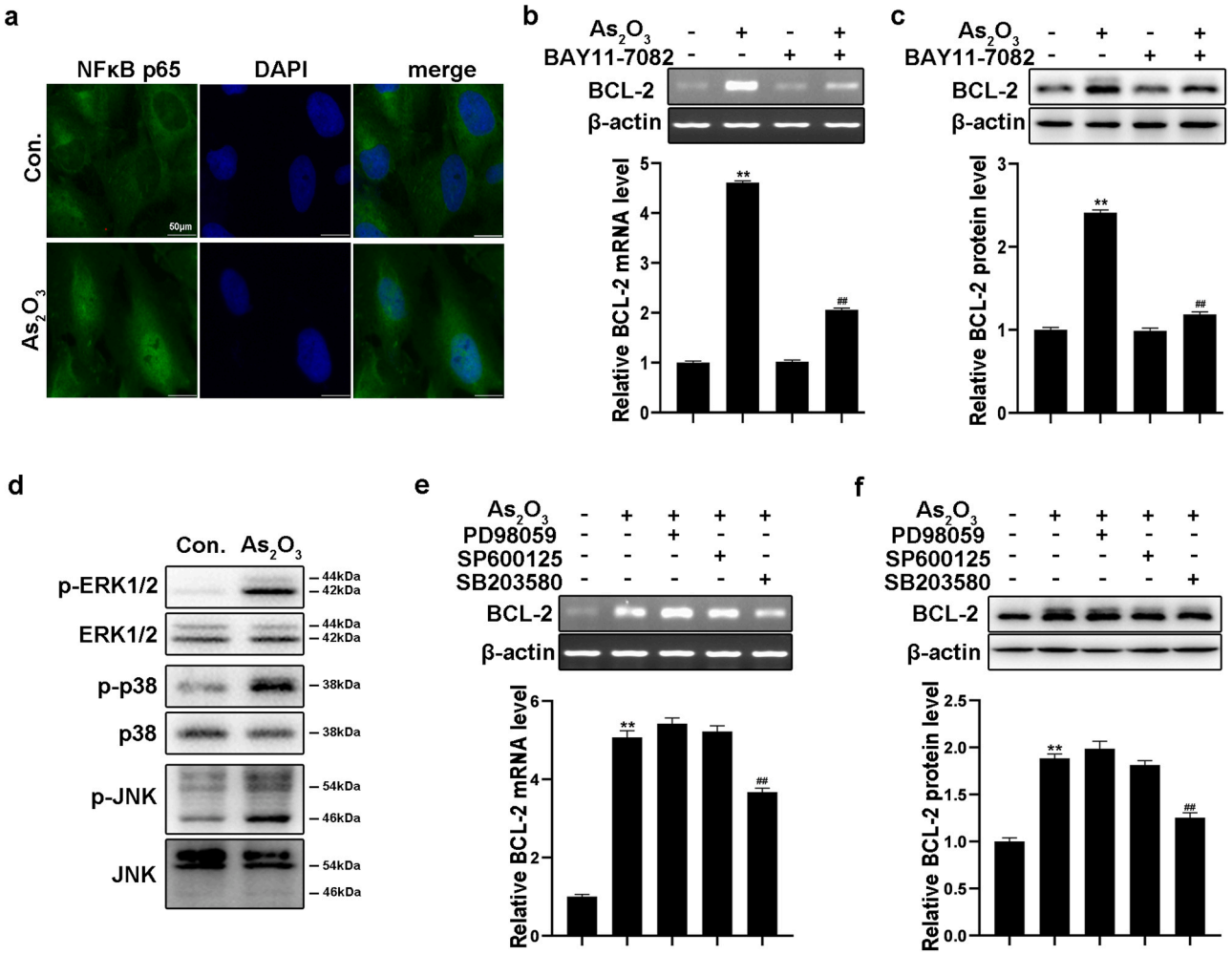

Fig. 3. Upregulation of BCL-2 expression by As_2O_3 through NF-κB activation and the p38 MAPK pathway in BEAS-2B cells. a. BEAS-2B cells were incubated with or without 2.0 μM As_2O_3 for 6 h, and they were stained with anti-NF-κB antibody and DAPI. Green fluorescence represents NF-κB and blue fluorescence represents nuclear DAPI staining. The bar represents 50 μm. b and c. BEAS-2B cells pretreated with 10 μM BAY11–7082 for 30 min, were incubated with or without 2.0 μM As_2O_3 for 24 h. Levels of BCL-2 mRNA (b) and protein (c) expression were measured using semi-quantitative RT-PCR analysis and Western blotting analysis, respectively. d. BEAS-2B cells were incubated with 2.0 μM of As_2O_3 for 24 h. Cell lysates were prepared and subjected to SDS-PAGE followed by immunoblotting using anti-p-ERK, anti-ERK, anti-p-p38 MAPK, anti-p38 MAPK, anti-p-JNK, and anti-JNK antibodies. e and f. BEAS-2B cells pretreated with 20 μM PD98059, 25 μM SP600125 or 10 μM SB203580 for 30 min were incubated with or without 2.0 μM As_2O_3 for 24 h. The levels of BCL-2 mRNA (e) and protein (f) expressions were measured by semi-quantitative RT-PCR analysis and Western blotting analysis, respectively. The band intensities representing BCL-2 protein expression levels were quantitated using the Image J Gel Analysis program and normalized by the intensity of the β-actin internal control. $^{**}p < 0.01$, significantly different from the control group; $^{\#\#}p < 0.01$, significantly different from the As_2O_3-treatment group.

Western blotting. As_2O_3-induced elevation of cleaved caspase-3 was inhibited completely by NAC, and partially by BAY11–7082, SB25038, Act D, and CHX (Fig. 5b). NAC, BAY11–7082, and SB25038 reduced As_2O_3-induced nuclear shrinkage, chromatin condensation, and DNA fragmentation (Fig. 4a). ABT-199, a potent and selective BCL-2 inhibitor, partially restored the BEAS-2B cell viability after 24 h of As_2O_3 treatment (Fig. 5c). Also, As_2O_3-induced cleaved caspase-3 was inhibited partially by ABT-199 (Fig. 5d). These results confirm that As_2O_3-induced BEAS-2B cell apoptosis is mediated by the upregulation of BCL-2 expression.

4. Discussion

In this study, we clarified that As_2O_3 increases BCL-2 expression, phosphorylation and the nuclear localization during apoptosis in BEAS-2B cells. Additionally, BCL-2 accumulation in the nucleus co-occurs with chromatin condensation induced by As_2O_3 in apoptotic cells.

Generally, in some certain types of cells, As_2O_3 dissociates the BCL-2/BAX heterodimer, and the downregulation of BCL-2 by the intrinsic apoptosis pathway is considered as one of the significant mechanisms in As_2O_3-induced apoptosis (Akao et al., 2000; Rana, 2008). However, in this study, expression levels of BCL-2 mRNA and protein are increased significantly at As_2O_3 doses that induced apoptosis in BEAS-2B cells. On the other hand, inhibition of expression and activity of BCL-2 by BAY11–7082, SB25038, Act D, CHX and ABT-199 showed mitigation of apoptosis in BEAS-2B cells. Shinoura et al. (1999) reported that the level of BCL-2 determines its anti-apoptotic or pro-apoptotic function. In particular, BCL-2 at a low expression level functions as anti-apoptotic, whereas BCL-2 at a high level of expression was proapoptotic to Fas-mediated apoptosis. Transient overexpression of BCL-2 protein results in potent apoptosis in MCF7 and 293 cell lines (Uhlmann et al., 1998). In MCF-7 cells, knockdown of BCL-2 gene delayed aspirin-induced apoptosis, while overexpression of BCL-2 gene promoted aspirin-induced apoptosis (Choi et al., 2013). These results, including our findings, indicate that the high level of BCL-2 expression in some types of cells is associated with apoptosis. However, we observed decreased protein expression of BCL-2 in RAW246.7 cells after treated with the apoptotic dose of As_2O_3 (Supplementary Fig. 1).

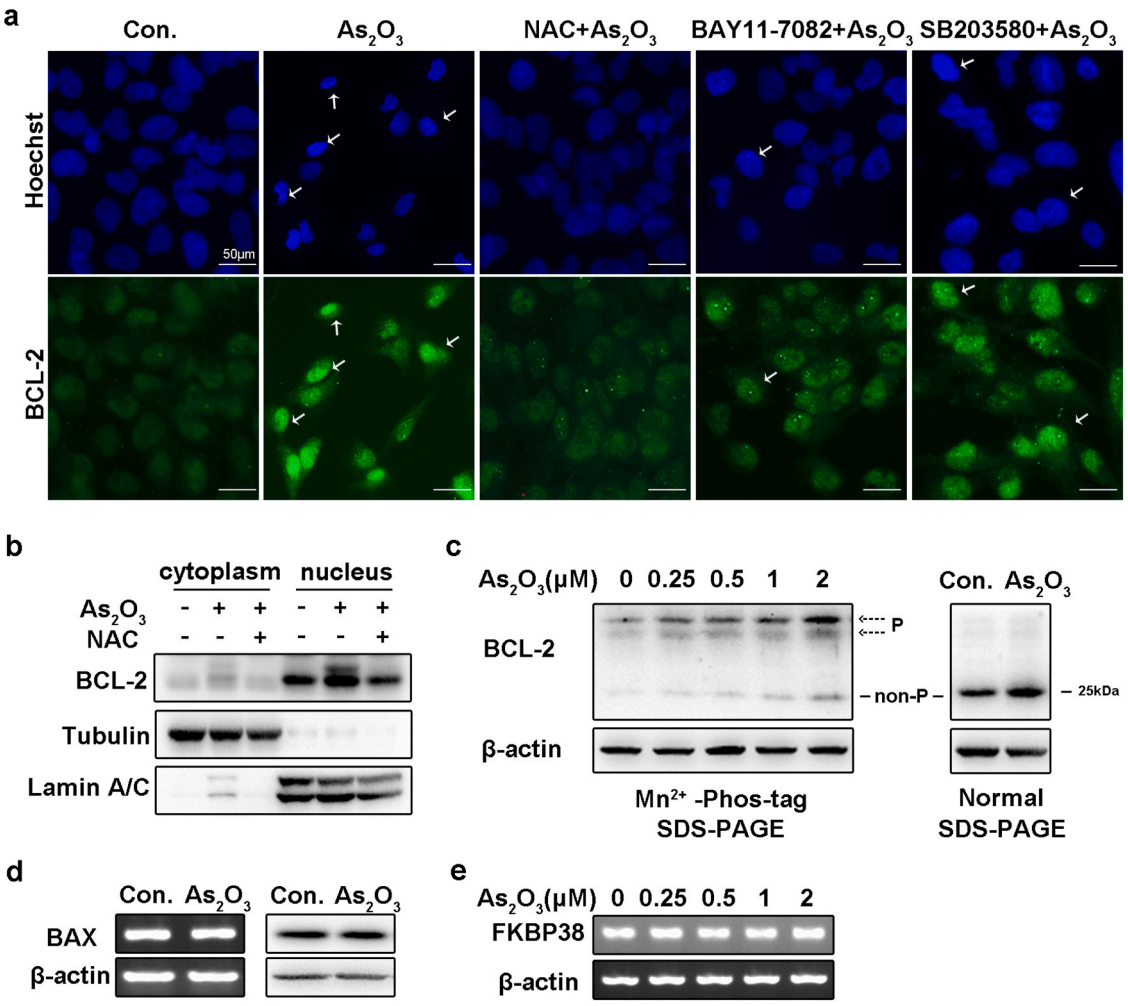

Fig. 4. The newly synthesized BCL-2 protein and its phosphorylation induced by As_2O_3 is located at the nucleus and associated with apoptotic chromatin condensation. a. BEAS-2B cells were stained with an anti-BCL-2 antibody and Hoechst 33342 after pretreatment with 5.0 mM NAC, 10 μM BAY11–7082, or 10 μM SB203580 for 30 min, and incubated with or without 2.0 μM As_2O_3 for 24 h. Green fluorescence represents BCL-2 and blue fluorescence represents nuclear Hochest 33342 staining. The bar represents 50 μm. Arrows indicate shrunken, condensed, and/or fragmented nuclei in apoptotic cells. b. BEAS-2B cells pretreated with 5.0 mM NAC for 30 min, were incubated with or without 2.0 μM As_2O_3 for 24 h; the cells were then disrupted and separated into cytoplasmic fractions and nuclear fractions. The BCL-2 protein in cytoplasmic and nuclear fractions was detected using Western blotting. Lamin A/C was used as the marker for the nuclear fraction, and tubulin was used as the marker for the cytoplasmic fraction. c. BEAS-2B cells were incubated with the indicated concentrations of As_2O_3 for 24 h. Cell lysates were analyzed by Phos-tag SDS-PAGE (left panels) and conventional SDS-PAGE (right panels) followed by Western blotting using anti-BCL-2 antibody. P: phosphorylated; non-P: non-phosphorylated. d. BEAS-2B cells were incubated with 2.0 μM As_2O_3 for 24 h, the expression of BAX mRNA and protein was detected using semi-quantitative RT-PCR and Western blotting, respectively. e. BEAS-2B cells were incubated with indicated concentrations of As_2O_3 for 24 h, and the expression of FKBP38 mRNA was measured using semi-quantitative RT-PCR analysis. Con, control.

Therefore, the antiapoptotic or pro-apoptotic function of BCL-2 may depend on the cell line. Previous studies have suggested that BCL-2 protein is located on the outer membrane of mitochondria, endoplasmic reticulum and nuclear envelope. However, our results showed that BCL-2 protein was mostly localized to the nucleus of BEAS-2B cells treated with or without As_2O_3 using both Western blot analysis of isolated nuclear fractions and immunostaining with two antibodies, 12789–1-AP (Proteintech) and GTX100064 (GeneTex). Our findings are in agreement with other reports that BCL-2 exists in the nuclei of mammalian cells (Hoetelmans et al., 2000; Yamamoto et al., 2001). The intense staining of BCL-2 in the nucleus of BEAS-2B cell induced by As_2O_3 is consistent with impaired chromatin condensation. Earlier studies have shown that the complex consisting of FKBP38 and BCL-2 is anchored to mitochondria and inhibits apoptosis. Knockdown of FKBP38 not only changes the subcellular localization of BCL-2, but also affects its anti-apoptotic activity (Shirane and Nakayama, 2003). The insufficient amount of FKBP38 may not interact effectively with the overexpressed BCL-2 and makes BCL-2 translocate from the cytoplasm to nucleus. Once BCL-2 is transported into the nucleus, it blocks transcription factors and initiates apoptosis due to a reduction of transcription factor activity (Massaad et al., 2004; Portier and Taglialatela, 2006). Nuclear BCL-2 was detected in the hippocampus and cerebellum of aged rats, which failed to protect cells from apoptosis induced by oxidative stress (Kaufmann et al., 2001). In this study, we found that As_2O_3 did not change FKBP38 mRNA expression, whereas BCL-2 expression was increased significantly and shuttled into the nucleus after As_2O_3 exposure (Fig. 4b and e). The localization of BCL-2 in the nucleus may decrease the activity of several transcription factors and induce apoptosis in BEAS-2B cells.

The phosphorylation sites are located in a nonstructural loop that links BH3 domain and BH4 domain of BCL-2 protein. The BCL-2 molecule at threonine-56, threonine-69, serine-70 and serine-87 are phosphorylated by some drugs (Blagosklonny, 2001; Srivastava et al., 1999; Yamamoto et al., 1999; Shitashige et al., 2001). In this study, we found BEAS-2B cells treated with As_2O_3 produced two upper bands of BCL-2 when assessed by Phos-tag-SDS-PAGE and immunoblotting. The level

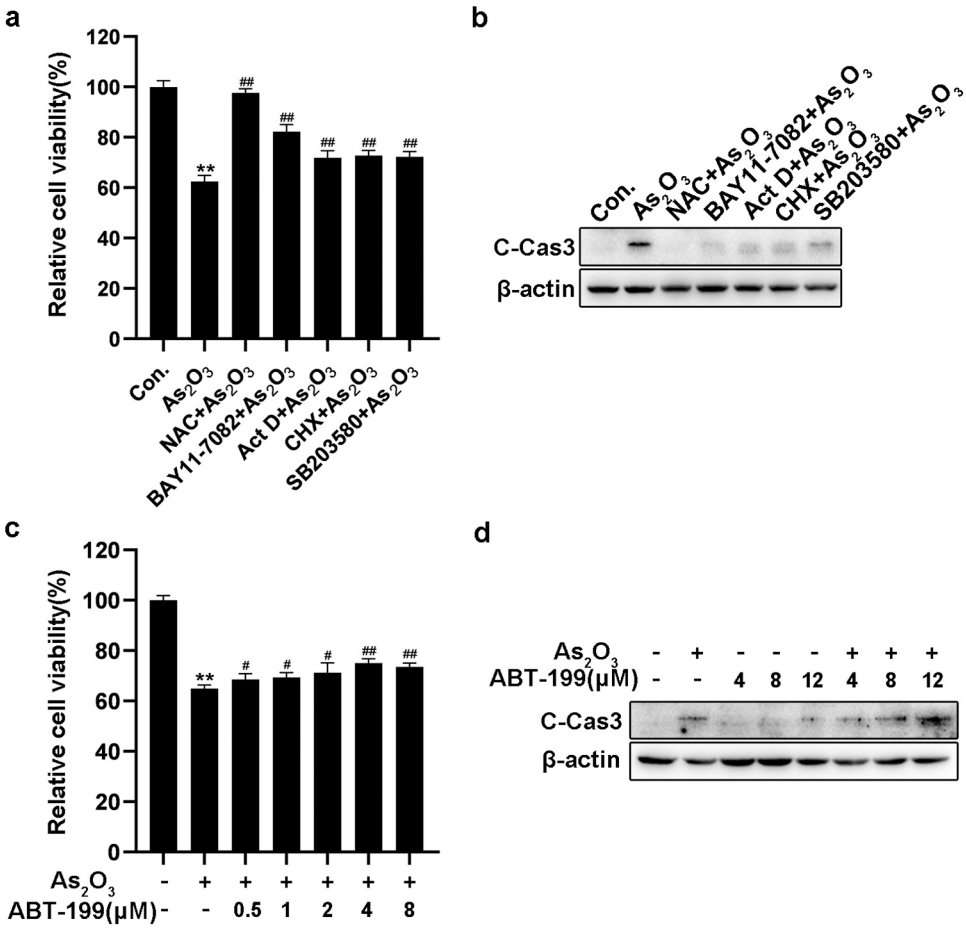

Fig. 5. Inhibition of As_2O_3-induced BCL-2 expression improves the viability of BEAS-2B cells. a. BEAS-2B cells pretreated with 5.0 mM NAC, 10 μM BAY11–7082, 2 μg/mL Act D, 10 μM CHX, or 10 μM SB203580 for 30 min were incubated in the presence of 2.0 μM As_2O_3 for 24 h. Cell viability was measured using a CCK-8 assay. Data were shown as the mean ± SEM of 3 independent experiments. b. BEAS-2B cells pretreated with 5.0 mM NAC, 10 μM BAY11–7082, 2 μg/mL Act D, 10 μM CHX, or 10 μM SB203580 for 30 min were incubated in the presence of 2.0 μM As_2O_3 for 24 h. Cell lysates were subjected to SDS-PAGE. Immunoblotting was carried out using anti-cleaved-caspase 3 antibody. c. BEAS-2B cells pretreated with indicated concentration of ABT-199 for 30 min were incubated in the presence of 2.0 μM As_2O_3 for 24 h. Cell viability was measured using a CCK-8 assay. Data were shown as the mean ± SEM of 3 independent experiments. d. BEAS-2B cells were pretreated with the indicated concentration of ABT-199 for 30 min, then incubated in the presence of 2.0 μM As_2O_3 for 24 h. Cell lysates were subjected to SDS-PAGE. Immunoblotting was carried out using an anti-cleaved-caspase 3 antibody. Act D, actinomycin D; CHX, cycloheximide; C-Cas 3, cleaved-caspase 3; Con, control. $^{**}p < 0.01$, compared to the control group; $^{\#}p < 0.05$ and $^{\#\#}p < 0.01$, compared to the As_2O_3-treatment group.

of BCL-2 phosphorylation is correlated with As_2O_3 concentration. Because deletion of the loop region of BCL-2 completely blocks the drug-induced apoptosis, phosphorylation of BCL-2 may be associated with its nuclear translocation and inactivation (Asnaghi et al., 2004; Srivastava et al., 1999).

Previous studies have demonstrated that transcription factor NF-κB binds to BCL-2 promoter and upregulates BCL-2 gene transcription in different types of cells (Tamatani et al., 1999; Catz and Johnson, 2001; Heckman et al., 2002). We have shown that when BEAS-2B cells were treated with 2.0 μM As_2O_3, NF-κB was translocated from the cytoplasm to nucleus, and As_2O_3-induced BCL-2 mRNA and protein expression were inhibited by NF-κB inhibitors. As_2O_3-induced NF-κB nuclear translocation is consistent with the results of researches on some types of cells (Li et al., 2002; Ganapathy et al., 2014; Chen et al., 2016). However, no correlation has been demonstrated between As_2O_3-induced NF-κB nuclear translocation and BCL-2 expression in any cell lines. Our results demonstrated that As_2O_3 induces the upregulation of BCL-2 mRNA and protein levels via the NF-κB pathway in BEAS-2B cells. Therefore, BCL-2 expression induced by As_2O_3 through the NF-κB pathway may be cell-dependent.

Other studies verified that BCL-2 expression is regulated by the MAPK family's ERK1/2, JNK and p38 MAPK (Subramanian and Shaha, 2007; Zhang et al., 2010). Here, we found that, although As_2O_3 activated the ERK, JNK, and p38 MAPK pathways, BCL-2 mRNA and protein expression were upregulated only by the p38 MAPK pathway, not by the ERK and JNK pathways.

Act D and CHX, as inhibitors of transcription and translation inhibited the upregulation of BCL-2 expression and its phosphorylation in paclitaxel-treated DND39 cells, and increased cell viability to the same level as that of control cells which did not express BCL-2 (Shitashige et al., 2001). In this study, we found that the upregulation of BCL-2 mRNA and protein expression in As_2O_3-treated BEAS-2B cells was associated with apoptosis. Act D, CHX, and the NF-κB inhibitor could inhibit the upregulation of BCL-2 and partially restore cell viability after As_2O_3 exposure.

In conclusion, we have provided strong experimental evidence that As_2O_3 induces the upregulation of BCL-2 expression, phosphorylation and nuclear localization, leading to apoptosis of BEAS-2B cells. In the mechanism explored in the present study, the NF-κB and p38 MAPK pathways are responsible for As_2O_3-induced upregulation of BCL-2 expression, as schematically illustrated in Fig. 6. BCL-2 is shuttled into the nucleus, and nuclear accumulation and phosphorylation of BCL-2 protein provides a functional link to apoptosis. Even though this phenomenon may be cell-dependent, our results provide a novel insight into the molecular mechanism of BCL-2-induced apoptosis. However, further studies are needed to explain how BCL-2 enters into the nucleus and induces apoptosis by arsenite and whether arsenite can induce apoptosis of the BEAS-2B cells through the extrinsic pathway.

CRediT authorship contribution statement

Jing Tang: Investigation, Data curation. **Chenjuan Yao:** Validation, Formal analysis. **Yingqi Liu:** Investigation, Validation. **Jiaming Yuan:** Investigation. **Li Wu:** Writing – review & editing. **Kazuo Hosoi:** Writing – review & editing. **Shali Yu:** Validation. **Chunyan Huang:** Formal analysis, Funding acquisition. **Haiyan Wei:** Conceptualization, Project administration, Writing – original draft, Funding acquisition. **Gang Chen:** Conceptualization, Writing – review & editing, Supervision.

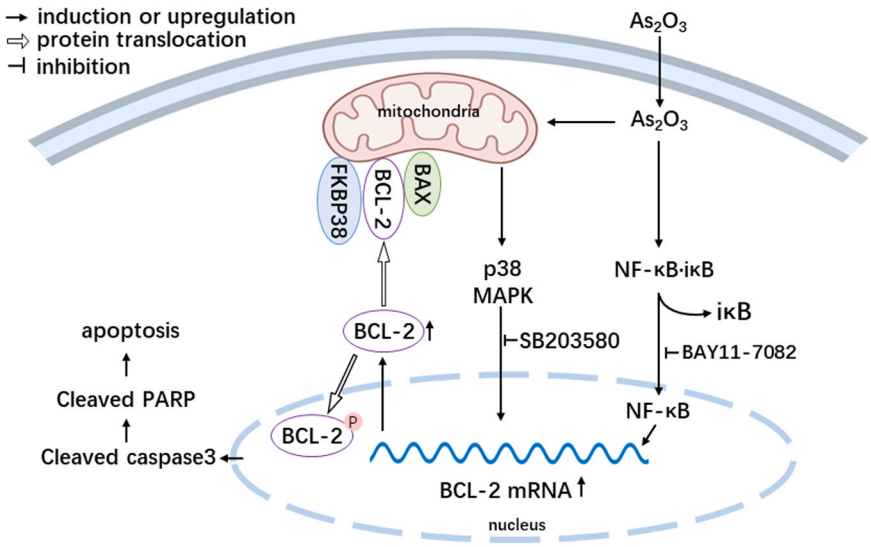

Fig. 6. A proposed model for As_2O_3-induced apoptosis of BEAS-2B cells showing the involvement of BCL-2 expression and nuclear translocation. As_2O_3 induces NF-κB transportation into the nucleus. The NF-κB and p38 MAPK signaling pathways upregulate the expression of BCL-2 mRNA and protein. Because of insufficient FKBP38, BCL-2 in the cytoplasm is shuttled into the nucleus, where it blocks transcription factor activity and initiates apoptosis due to the decreased transcription factor activity.

Declaration of Competing Interest

The authors declare that they have no known competing financial interests or personal relationships that could have appeared to influence the work reported in this paper.

Acknowledgments

This study was supported by the Provincial Undergraduate Innovation Experiment Project (grant number 202010304105Y), the Key Technology Research and Development Program of Jiangsu Province (grant number BE2019674), the Science and Technology Planning Project of Suzhou (grant number SYS2020197) and Large Instruments Open Foundation of Nantong University (grant number KFJN2049).

Appendix A. Supporting information

Supplementary data associated with this article can be found in the online version at doi:10.1016/j.ecoenv.2021.112531.

References

Abdul, K.S., Jayasinghe, S.S., Chandana, E.P., Jayasumana, C., De Silva, P.M., 2015. Arsenic and human health effects: a review. Environ. Toxicol. Pharmacol. 40, 828–846.
Akao, Y., Yamada, H., Nakagawa, Y., 2000. Arsenic-induced apoptosis in malignant cells in vitro. Leuk. Lymphoma 37, 53–63.
Asnaghi, L., Calastretti, A., Bevilacqua, A., D'Agnano, I., Gatti, G., Canti, G., Delia, D., Capaccioli, S., Nicolin, A., 2004. Bcl-2 phosphorylation and apoptosis activated by damaged microtubules require mTOR and are regulated by Akt. Oncogene 23, 5781–5791.
Banerjee, N., Banerjee, M., Ganguly, S., Bandyopadhyay, S., Das, J.K., Bandyopadhay, A., Chatterjee, M., Giri, A.K., 2008. Arsenic-induced mitochondrial instability leading to programmed cell death in the exposed individuals. Toxicology 246, 101–111.
Blagosklonny, M.V., 2001. Unwinding the loop of Bcl-2 phosphorylation. Leukemia 15, 869–874.
Carneiro, B.A., El-Deiry, W.S., 2020. Targeting apoptosis in cancer therapy. Nat. Rev. Clin. Oncol. 17, 395–417.
Catz, S.D., Johnson, J.L., 2001. Transcriptional regulation of bcl-2 by nuclear factor kappa B and its significance in prostate cancer. Oncogene 20, 7342–7351.
Chen, G., Mao, J., Zhao, J., Zhang, Y., Li, T., Wang, C., Xu, L., Hu, Q., Wang, X., Jiang, S., Nie, X., Wu, Q., 2016. Arsenic trioxide mediates HAPI microglia inflammatory response and the secretion of inflammatory cytokine IL-6 via Akt/NF-kappaB signaling pathway. Regul. Toxicol. Pharmacol. 81, 480–488.
Choi, B.H., Chakraborty, G., Baek, K., Yoon, H.S., 2013. Aspirin-induced Bcl-2 translocation and its phosphorylation in the nucleus trigger apoptosis in breast cancer cells. Exp. Mol. Med. 45, 47.
Czabotar, P.E., Lessene, G., Strasser, A., Adams, J.M., 2014. Control of apoptosis by the BCL-2 protein family: implications for physiology and therapy. Nat. Rev. Mol. Cell Biol. 15, 49–63.
Dua, T.K., Dewanjee, S., Khanra, R., 2016. Prophylactic role of Enhydra fluctuans against arsenic-induced hepatotoxicity via anti-apoptotic and antioxidant mechanisms. Redox Rep. 21, 147–154.
Edison, N., Curtz, Y., Paland, N., Mamriev, D., Chorubczyk, N., Haviv-Reingewertz, T., Kfir, N., Morgenstern, D., Kupervaser, M., Kagan, J., Kim, H.T., Larisch, S., 2017. Degradation of Bcl-2 by XIAP and ARTS promotes apoptosis. Cell Rep. 21, 442–454.
Ganapathy, S., Xiao, S., Seo, S.J., Lall, R., Yang, M., Xu, T., Su, H., Shadfan, M., Ha, C.S., Yuan, Z.M., 2014. Low-dose arsenic induces chemotherapy protection via p53/NF-kappaB-mediated metabolic regulation. Oncogene 33, 1359–1366.
Haldar, S., Chintapalli, J., Croce, C.M., 1996. Taxol induces bcl-2 phosphorylation and death of prostate cancer cells. Cancer Res. 56, 1253–1255.
Hanson, C.J., Bootman, M.D., Distelhorst, C.W., Maraldi, T., Roderick, H.L., 2008. The cellular concentration of Bcl-2 determines its pro- or anti-apoptotic effect. Cell Calcium 44, 243–258.
Heckman, C.A., Mehew, J.W., Boxer, L.M., 2002. NF-kappaB activates Bcl-2 expression in t(14;18) lymphoma cells. Oncogene 21, 3898–3908.
Hoetelmans, R., van Slooten, H.J., Keijzer, R., Erkeland, S., van de Velde, C.J., Dierendonck, J.H., 2000. Bcl-2 and bax proteins are present in interphase nuclei of mammalian cells. Cell Death Differ. 7, 384–392.
Hughes, M.F., Beck, B.D., Chen, Y., Lewis, A.S., Thomas, D.J., 2011. Arsenic exposure and toxicology: a historical perspective. Toxicol. Sci. 123, 305–332.
Kaufmann, J.A., Bickford, P.C., Taglialatela, G., 2001. Oxidative-stress-dependent up-regulation of Bcl-2 expression in the central nervous system of aged Fisher-344 rats. J. Neurochem. 76, 1099–1108.
King, Y.A., Chiu, Y.J., Chen, H.P., Kuo, D.H., Lu, C.C., Yang, J.S., 2016. Endoplasmic reticulum stress contributes to arsenic trioxide-induced intrinsic apoptosis in human umbilical and bone marrow mesenchymal stem cells. Environ. Toxicol. 31, 314–328.
Kinoshita, E., Kinoshita-Kikuta, E., Koike, T., 2009. Separation and detection of large phosphoproteins using Phos-tag SDS-PAGE. Nat. Protoc. 4, 1513–1521.
Kumar, S., Yedjou, C.G., Tchounwou, P.B., 2014. Arsenic trioxide induces oxidative stress, DNA damage, and mitochondrial pathway of apoptosis in human leukemia (HL-60) cells. J. Exp. Clin. Cancer Res. 33, 42.
Li, M., Cai, J.F., Chiu, J.F., 2002. Arsenic induces oxidative stress and activates stress gene expressions in cultured lung epithelial cells. J. Cell Biochem. 87, 29–38.
Liu, J., Zheng, B., Aposhian, H.V., Zhou, Y., Chen, M.L., Zhang, A., Waalkes, M.P., 2002. Chronic arsenic poisoning from burning high-arsenic-containing coal in Guizhou, China. Environ. Health Perspect. 110, 119–122.
Liu, Y., Tang, J., Yuan, J., Yao, C., Hosoi, K., Han, Y., Yu, S., Wei, H., Chen, G., 2020. Arsenite-induced downregulation of occludin in mouse lungs and BEAS-2B cells via the ROS/ERK/ELK1/MLCK and ROS/p38 MAPK signaling pathways. Toxicol. Lett. 332, 146–154.
Massaad, C.A., Portier, B.P., Taglialatela, G., 2004. Inhibition of transcription factor activity by nuclear compartment-associated Bcl-2. J. Biol. Chem. 279, 54470–54478.
Portier, B.P., Taglialatela, G., 2006. Bcl-2 localized at the nuclear compartment induces apoptosis after transient overexpression. J. Biol. Chem. 281, 40493–40502.
Rahman, M.M., Uson-Lopez, R.A., Sikder, M.T., Tan, G., Hosokawa, T., Saito, T., Kurasaki, M., 2018. Ameliorative effects of selenium on arsenic-induced cytotoxicity in PC12cells via modulating autophagy/apoptosis. Chemosphere 196, 453–466.
Rana, S.V., 2008. Metals and apoptosis: recent developments. J. Trace Elem. Med. Biol. 22, 262–284.
Shinoura, N., Yoshida, Y., Nishimura, M., Muramatsu, Y., Asai, A., Kirino, T., Hamada, H., 1999. Expression level of Bcl-2 determines anti- or proapoptotic function. Cancer Res. 59, 4119–4128.
Shirane, M., Nakayama, K.I., 2003. Inherent calcineurin inhibitor FKBP38 targets Bcl-2 to mitochondria and inhibits apoptosis. Nat. Cell Biol. 5, 28–37.
Shitashige, M., Toi, M., Yano, T., Shibata, M., Matsuo, Y., Shibasaki, F., 2001. Dissociation of Bax from a Bcl-2/Bax heterodimer triggered by phosphorylation of serine 70 of Bcl-2. J. Biochem. 130, 741–748.

Siddiqui, W.A., Ahad, A., Ahsan, H., 2015. The mystery of BCL2 family: Bcl-2 proteins and apoptosis: an update. Arch. Toxicol. 89, 289–317.
Singh, R., Letai, A., Sarosiek, K., 2019. Regulation of apoptosis in health and disease: the balancing act of BCL-2 family proteins. Nat. Rev. Mol. Cell Biol. 20, 175–193.
Srivastava, R.K., Srivastava, A.R., Korsmeyer, S.J., Nesterova, M., Cho-Chung, Y.S., Longo, D.L., 1998. Involvement of microtubules in the regulation of Bcl2 phosphorylation and apoptosis through cyclic AMP-dependent protein kinase. Mol. Cell Biol. 18, 3509–3517.
Srivastava, R.K., Mi, Q.S., Hardwick, J.M., Longo, D.L., 1999. Deletion of the loop region of Bcl-2 completely blocks paclitaxel-induced apoptosis. Proc. Natl. Acad. Sci. U.S.A. 96, 3775–3780.
Subramanian, M., Shaha, C., 2007. Up-regulation of Bcl-2 through ERK phosphorylation is associated with human macrophage survival in an estrogen microenvironment. J. Immunol. 179, 2330–2338.
Tamatani, M., Che, Y.H., Matsuzaki, H., Ogawa, S., Okado, H., Miyake, S., Mizuno, T., Tohyama, M., 1999. Tumor necrosis factor induces Bcl-2 and Bcl-x expression through NFkappaB activation in primary hippocampal neurons. J. Biol. Chem. 274, 8531–8538.
Taylor, R.C., Cullen, S.P., Martin, S.J., 2008. Apoptosis: controlled demolition at the cellular level. Nat. Rev. Mol. Cell Biol. 9, 231–241.
Uhlmann, E.J., Subramanian, T., Vater, C.A., Lutz, R., Chinnadurai, G., 1998. A potent cell death activity associated with transient high level expression of BCL-2. J. Biol. Chem. 273, 17926–17932.
Wang, H.Q., Nakaya, Y., Du, Z., Yamane, T., Shirane, M., Kudo, T., Takeda, M., Takebayashi, K., Noda, Y., Nakayama, K.I., Nishimura, M., 2005. Interaction of presenilins with FKBP38 promotes apoptosis by reducing mitochondrial Bcl-2. Hum. Mol. Genet. 14, 1889–1902.
WHO, 2001. Arsenic and Arsenic Compounds. In: Environmental Health Criteria, , 2nd Ed.224. World Health Organization, Geneva.
Yamamoto, K., Ichijo, H., Korsmeyer, S.J., 1999. BCL-2 is phosphorylated and inactivated by an ASK1/Jun N-terminal protein kinase pathway normally activated at G(2)/M. Mol. Cell Biol. 19, 8469–8478.
Yamamoto, K., Ladage, P.M., Ren, D.H., Li, L., Petroll, W.M., Jester, J.V., Cavanagh, H. D., 2001. Bcl-2 expression in the human cornea. Exp. Eye Res. 73, 247–255.
Zhang, C.L., Song, F., Zhang, J., Song, Q.H., 2010. Hypoxia-induced Bcl-2 expression in endothelial cells via p38 MAPK pathway. Biochem Biophys. Res. Commun. 394, 976–980.